Light Amplification and Nonlinear Microscopy by Stimulated Raman Scattering

M. A. Ferrara[1], A. D'Arco[1,2], M. Indolfi[1], N. Brancati[3], L. Zeni[2] and L. Sirleto[1]

[1]*National Research Council (CNR) - Institute for Microelectronics and Microsystems, I-80131 Napoli, Italy*
[2]*Second University of Naples (SUN), Department of Information Engineering, I-81031 Aversa, Italy*
[3]*National Research Council (CNR) – Istituto di Calcolo e Reti ad Alte Prestazioni, I-80131 Napoli, Italy*

Abstract: The Stimulated Raman Scattering has important connections with nanophotonics and biophotonics. Concerning nanophotonics, one of the most recent challenges is the investigation of 'nonlinear optical phenomena at nanoscale'. Among them, stimulated Raman scattering is one of the most interesting, due to its significant implications from both fundamental and applicative point of view. In this paper, comparison among experimental investigations of stimulated Raman scattering in amorphous silicon nanoparticles and in silicon micro- and nano-crystals, at the wavelengths of interest for telecommunications, are reported. In addition, concerning biophotonics, first, the implementation of femtosecond Stimulated Raman Spectroscopy (f-SRS), as a single point of scanning microscopy, is described. Then, the integration of f-SRS in a laser scanning microscope and label free imaging of polystyrene-beads are demonstrated.

1 INTRODUCTION

In silicon photonics and silicon nanophotonics, amplification and light emission are still the most challenging goals to get. In Stimulated Raman Scattering (SRS), a pump laser beam enters a nonlinear medium and spontaneous generation and amplification lead to a beam at a frequency different from the pump. Raman amplification, demonstrated in the early 1970s, is an interesting approach for optical amplification, because it is only restricted by the pump wavelength and Raman active modes of the gain medium (Shen and Bloembergen, 1965).

Raman lasing can be achieved by using SRS phenomenon, which permits, in principle, the amplification in a wide interval of wavelengths, from the ultraviolet to the infrared (Stolen, 2004). SRS is used in tunable laser development, high energy pulse compression, etc. Considering bulk semiconductors, lasing by SRS was first discovered in GaP (Nishizawa and Suto, 1980), whereas SRS from spherical droplets and microspheres, with diameters 5-20 µm, has been observed using both pulsed and continuous wave probe beams (Spillane *et al.*, 2002). Raman lasers have been also demonstrated in silicon micro-waveguides (Rong *et al.*, 2005).

The "ideal" material for Raman amplification should have wide, flat and high Raman gain into all the range of interest in telecommunications (from 1270 to 1650 nm). Unfortunately, as a general rule, due to the physics behind the Raman effect, there is a tradeoff for Raman amplification. In nature, we have material, for example silicon, with high Raman efficiency and small bandwidth, and material, for example silica, with a large bandwidth but with small amplification (see figure 1). The above-mentioned tradeoff is a fundamental limitation towards the realization of micro-/nano-sources with large emission spectra. Therefore, the investigation of new materials possessing both large Raman gain coefficients and spectral bandwidth is becoming mandatory in order to satisfy the increasing telecommunications demands (Refi, 1999). In order to overcome these limitations, a possible option is to consider nanocomposite and nanostructured materials.

Raman scattering in electrons-confined and photons confined materials is a fascinating research field of great importance from both fundamental and applicative point of view. Concerning the fundamental one, there have been a number of investigations both experimental and theoretical, but the question is still "open" (Gaponenko *et al.*, 2002), while from an applicative point of view, there are

some important prospective, for example to realize micro/nano source, with improved performances, based on SRS.

The phenomenon of strong resonant and local enhancement of visible electro-magnetic (EM) radiation when incident on the surface of metallic particles and films resulting from surface plasmon resonances, continues to attract significant attention for fundamental and applied interests (Kawata, 2009). However, the possibility of EM radiation enhancement from semiconducting and insulating materials, particularly in silicon, is noteworthy for silicon-based optoelectronic applications owing to the potential for monolithically integrating photonic technology and semiconductor electronics (Cao *et al.*, 2006). Except for a report of SRS from individual single walled carbon nanotubes (Zhang *et al.*, 2006), and the observation of SRS from semiconductor nanowires (Wu *et al.*, 2009), we find no other evidence for this important nonlinear optic effect in nanostructured materials.

In biophotonics, confocal and multiphotons fluorescence microscopy are important and powerful techniques for imaging of biological samples. However, these microscopic techniques show some limitations, indeed, they require chemical labels that could interfere with biological functionalities; additionally the photo-bleaching introduces artefacts and limits the measurement repeatability. Therefore, it is necessary to introduce and implement a new multiphotons microscopy technique suited for real time imaging with high three dimensional spatial resolution and chemical specificity of unlabeled living cells. Raman microscopy can be used as a contrast mechanism based on vibrational properties. A typical Raman spectrum makes available information on the molecular and chemical structure of the sample, offering an intrinsic chemical selectivity. Nevertheless, linear Raman microscopy is limited to weak signals, so, to obtain an image acquisition times are very long.

It is worth noting that, due to the recent femtoseconds laser technological development, nonlinear techniques have found application in soft matter and in particular in biological materials. Femtoseconds laser allows to obtain an average power, incident onto the sample, lower than the photodamage limit and a high enough pump peak power to ensure the triggering of the nonlinear effects. In addition, the range of pulses wavelengths, generated into the range between 680 nm and 1300 nm, permits to work in the window of water transparency, significantly reducing the absorption. Coherent Raman Scattering (CRS) techniques are sensitive to the same molecular vibrations probed in spontaneous Raman spectroscopy, but unlike linear Raman spectroscopy, CRS techniques exhibit a nonlinear dependence on the incoming light fields and produce coherent radiation. In CRS, two collinear laser beams (pump and probe) at different frequencies excite the sample. When the difference in frequencies is equal to a molecular vibration, a stimulated and coherent excitation of molecular bond vibration modes (third order non-linear process) occur and a significant increase of Raman signal is observed. This latter property has popularized CRS as a microscopy modality, as it is intimately related to the technique's strong optical signals that enable fast imaging applications. CRS microscopy makes it possible to achieve images based on vibrational Raman contrast at imaging speeds much faster than attained with conventional Raman microscopes. Clearly, this attribute is very attractive for biological imaging, where imaging speed is an important experimental parameter (Ploetz *et al.*, 2007; Freudiger *et al.*, 2008; Ozeki *et al.*, 2009; Nandakumar *et al.*, 2009; Fu *et al.*, 2013).

CRS includes two techniques: coherent anti-Stokes Raman scattering (CARS) and SRS. We note that a CARS spectrum is different from its corresponding spontaneous Raman spectrum due to a non-resonant background, which complicates spectral assignment, causes difficulties in image interpretation, and limits detection sensitivity (Ploetz *et al.*, 2007; Freudiger *et al.*, 2008; Ozeki *et al.*, 2009; Nandakumar *et al.*, 2009).

The recent development of SRS microscopy overcame these limitations and provided better imaging contrast mechanism (vibrational) contrast. SRS eliminates the non-resonant background problem because the generated third order SRS nonlinear polarization is directly heterodyne mixed and amplified by the input beam with the exact same phase, therefore always resulting in a zero non-resonant contribution. Definitely, SRS is free from the non-resonant background, exhibiting an identical spectrum as the spontaneous Raman it is linearly proportional to the concentration of the analyte, and therefore it allows straightforward quantification. In such situations, it is natural to consider the application of SRS to biological microscopy. When SRS microscopy was proposed (Ploetz *et al.*, 2007; Freudiger *et al.*, 2008; Ozeki *et al.*, 2009), two transform-limited picosecond (ps) lasers with narrow spectral bandwidth were used to excite a single Raman-active vibrational mode for fast imaging with high spectral resolution. With this ps–ps excitation sources it is not possible to distinguish

mixed chemical species with overlapped Raman bands in the sample because other vibrational modes of the sample are not excited. However, in many live biological and biomedical applications, simultaneous mapping of different chemical species in the same sample is extremely important for the investigation of the co-distribution or dynamic correlation between pairs of biomolecules. Therefore, multicolor imaging with multiple chemical contrasts is considered necessary. We note that multicolor imaging can be realized only taking advantage of femtosecond laser source (Nandakumar *et al.*, 2009).

In this paper, in paragraph 2 a comparison between our experimental results of SRS obtained on different samples of nanostructured amorphous silicon clusters, and of silicon micro-crystals (Si-μc) and nano-crystals (Si-nc) are reported. The two main figure of merit (Raman gain and bandwidth) are compared to an ideal material and we highlight a possible trend to get the best performance.

In paragraph 3, the details of experimental set up and the main experimental issues of femtosecond Stimulated Raman Spectroscopy (f-SRS) implementation are reported. In addition, steps towards nonlinear microscopy, i.e. the integration of f-SRS in a laser scanning microscope, is described. Finally, label free imaging of polystyrene-beads are demonstrated.

2 LIGHT AMPLIFICATION BY STIMULATED RAMAN SCATTERING

In our previous papers (Sirleto *et al.*, 2004 and 2006; Ferrara *et al.*, 2008), some advantages of silicon nanostructure with respect to silicon were demonstrated. Experimental results, proving spontaneous Raman scattering in silicon nanostructures at the wavelength of interest for telecommunications (1.54 μm), were reported in Refs. (Sirleto *et al.*, 2004 and 2006; Ferrara *et al.*, 2008). According to phonon confinement model in Refs. (Sirleto *et al.*, 2004 and 2006; Ferrara *et al.*, 2008), two significant improvement of Raman approach in silicon quantum dots with respect to silicon were demonstrated: the broadening of spontaneous Raman emission and the tuning of the Stokes shift. Considering silicon quantum dots having crystal size of 2 nm, a significant broadening of about 65 cm^{-1} and a peak shift of about 19 cm^{-1} were obtained. Because the width of C-band telecommunication is 146 cm^{-1}, taking into account

the broadening and the shift of spontaneous Raman emission, more than the half of C-band could be cover using silicon quantum dots, without implementing the multi-pump scheme.

Nanocomposites are random media containing domains or inclusions that are on the nanometric size scale. The optical properties of composite materials can be adjusted by controlling the constituents and morphology of the composite structure. The optical nanocomposite approach offers opportunities to produce high-performance and relatively low-cost optoelectronic media suitable for many applications.

In our previous papers (Sirleto *et al.*, 2004 and 2006; Ferrara *et al.*, 2008), SRS has been measured using as pump a CW Raman laser operating at 1427 nm. SRS net gain (*G*) is given by:

$$G = \frac{10}{L} log_{10} \left(\frac{I_S(L)}{I_S(0)} \right) = 4.34 g I_P(0) \qquad (1)$$

where $I_p = P/A$, with *P* is the power incident onto the sample and *A* is the effective area of pump beam. Since the sample is transparent to the incident light, *L* is taken to be equal to the thickness of the sample along the path of the incident light. *G* as a function of signal laser wavelength was measured in three different samples:

- Silicon nanocomposites dispersed in SiO$_2$ matrix, with a probe signal at 1542.2nm (Sirleto *et al.*, 2009; Ferrara *et al.*, 2011). The mean radius of the silicon dots and the dot density were respectively of 49nm (Si-μc) and 1.62x10^8 dots/cm^2.
- Amorphous silicon nanoclusters embedded in Si-rich Nitride/Silicon superlattice structures (SRN/Si-SLs), with a probe signal at 1540.6nm (Sirleto *et al.*, 2008). The structure of the sample consists of 10 SRN layers and 9 amorphous Si (a-Si) layers for a total thickness of 450 nm. Amorphous silicon nanoclusters size was about 2nm.
- Silicon nanocrystals embedded in silica matrix, with a probe signal at 1541.3nm (Sirleto *et al.*, 2012). Si-nc size was about 4nm.

In particular, we focalized our study on two different nanocomposites materials based on amorphous or crystalline silicon. The difference between them is related to their different spontaneous Raman signal, indeed in amorphous silicon Raman spectra is broadband but shows a low intensity, while in crystalline silicon Raman spectra is very narrowband but shows a high intensity. Additionally, considering that Raman effect is a volume effect, in the sense that the greater is the

volume of interaction, the higher is the Raman signal, we aspect that different concentration of nanoparticles could lead to different Raman gain. Results obtained can be summarized as follows:

- In silicon nanocomposites, an amplification of Stokes signal up to 1.4 dB/cm is reported. This result showed a preliminary valuation of approximately a five-fold enhancement of the Raman gain with respect to bulk silicon. Moreover, a threshold power reduction of about 60% is also reported (Sirleto *et al.*, 2009, Ferrara *et al.*, 2011).

- In SRN/Si-SLs, amplification of Stokes signal up to 0.87 dB/cm was experimentally demonstrated, consistent with a preliminary valuation of approximately a four-fold enhancement of the Raman gain with respect to bulk silicon. Moreover, a threshold power reduction of about 40% is also reported (Sirleto *et al.*, 2008).

- A giant Raman gain from the silicon nanocrystals is obtained that is up to four orders of magnitude greater than in bulk crystalline silicon (Sirleto *et al.*, 2012).

In figure 1 the Raman Gain coefficients and their bandwidth for all the samples are reported and compared with an ideal material. We note that si-nc has a Raman gain value comparable to the ideal materials, but the bandwidth is still small. Probably if the nanostructures was embedded in a different matrix, a greater bandwidth could be obtained, too.
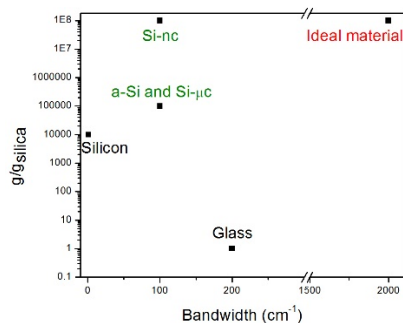
Figure 1: Raman Gain coefficients and their bandwidth are reported for different materials: silicon and silica (as 'bulk material'), and silicon micro- and nano-particles (amorphous and crystalline). Features for 'ideal materials' for Raman amplification are reported, too.

3 STIMULATED RAMAN MICROSCOPY

In SRS microscopy, pump and probe pulses at angular frequencies of ω_1 and ω_2 ($\omega_1 > \omega_2$) are focused into a sample, and the intensity change of the probe pulse due to SRS is detected. Intuitively, SRS is caused by the optical phase modulation induced by the time-dependent refractive index reflecting the molecular vibration, which is coherently driven by the intensity beat between pump and probe pulses (Shen and Bloembergen, 1965).

Concerning SRS, an important issue is its sensitivity, because the SRS signal is detected as a small change of the intensity of excitation beam, and hence is deteriorated by shot-noise and laser intensity noise. The laser intensity noise is quite important aspect to take into account in SRS microscopy because it can easily surpass the shot noise, an intrinsic property of the light source (Min *et al.*, 2011).

In the field of laser spectroscopy, SRS was extensively studied as a highly sensitive tool of vibrational spectroscopy (Owyoung, 1978) and the detection of SRS with a shot-noise limited sensitivity was achieved (Owyoung, 1978, Levine *et al.*, 1979; Heritage *et al.*, 1980). The basic idea is to take advantage of lock-in detection at high-frequency. In this approach, a high-frequency modulation transfer method to detect the signal is used. The intensity of the pump beam is modulated with an electro-optic modulator and the modulation transfered to the probe beam is measured with a lock-in amplifier (LIA) after blocking the pump beam with an optical filter. It is preferable to increase the modulation frequencies because the relative intensity noise of laser pulses typically decreases with frequency. Increasing modulation frequency of the beam, at frequencies above 1 MHz, it allows to reach the intrinsic limit of photodetectors. The thermal noise can be negligible compared to the shot noise when the optical power is of the order of several milliWatts.

Fig. 2 shows the schematic layout of the microscope; it requires two sources. The first one, used as a pump beam, is a femtosecond Ti-sapphire (Chameleon Ultra II) with a pulse duration of approximately 100 fs with a repetition rate of 80MHz and emission wavelengths into the range 680-1080nm. The second one, used as probe beam, is a femtosecond synchronized optical parametric oscillator (SOPO-Chameleon Compact OPO) with a pulse duration of approximately 200 fs with a repetition rate of 80MHz that emits into the range of wavelengths 1000-1600nm. An electro -optic modulator (EOM 350-160 KD*P CONOPTICS) was placed for the intensity modulation of the pump

pulses at a modulation frequency of 9.1 MHz. These two beams were collinearly combined with a dichroic mirror (Semrock FF875-Di01-25x36), temporally overlapped by a delay line (Newport MOD M-ILS200CC) and focused inside a sample through a scanning microscope (Ti-eclipse Nikon). The integration with the microscope ensures greater stability of the system and increase the spatial resolution of the measurement, while the presence of scanning unit allows the analysis on a large area, i.e. the realization of an image.
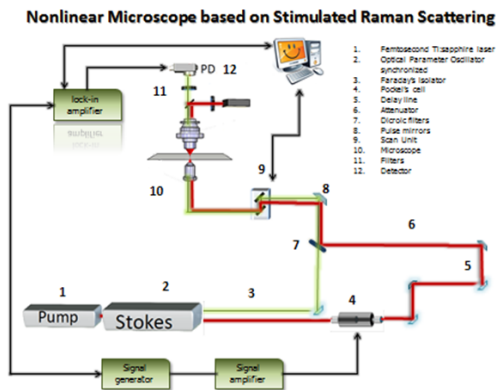
Figure 2: Experimental setup for SRS microscopy.

A 20X objective focuses beams inside a sample, and output pulses are collected by a 60X high numerical aperture objective. After, pump pulses are removed by a stack of optical filter, while probe pulses are detected by a photodetector (Thorlabs DET 10N/M) and measured by a lock-in amplifier (SR844- 200 MHz dual phase). The electrical signal coming out from the lock-in amplifier is digitalized by a PCI card, which manages and synchronizes the lock-in amplifier and the scanning unit of microscope in order to collect information and to obtain a 2D image.

A first measurement of stimulated Raman spectroscopy was carried out on a single point of a drop of a water solution with a very high density of polystyrene beads, which is placed between a microscope slide and a coverslip; the polystyrene beads had a diameter of 15μm. In order to investigate a typical C-H bond of polystyrene (Raman shift of 3054 cm^{-1}), the pump signal was set at 799 nm with a focused power of 20mW, while the probe signal was set at 1057nm with a focused power of 10mW. The temporal overlap of these two beams was obtained by scanning the delay line with steps of 0.001mm corresponding to 13,3fs time-shift. The time constant of the LIA was set to 3 ms with a slope of 18 dB/oct and 30μV sensitivity. The

measured values from lock-in amplifier, in terms of phase and amplitude of SRS signal as a function of the probe-pump delay in ps, are reported in Fig.3.
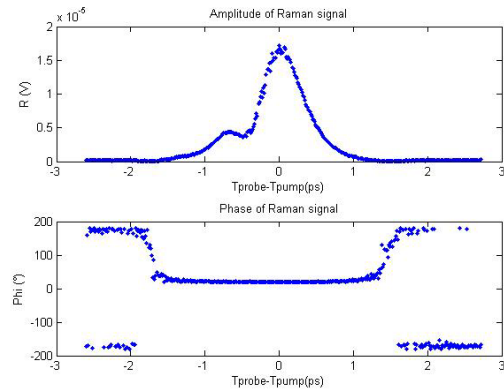
Figure 3: Amplitude and Phase of SRS signal measured by lock-in amplifier.

Because SRS uses near-infrared excitation light, the standard optics of a laser-scanning multiphoton microscope are compatible with SRS modalities. In particular, SRS uses the same high numerical aperture (NA) lenses that are employed in multiphoton microscopes. In fact, a SRS imaging modality shares many of the imaging properties of a multiphoton microscope, including fast image acquisition and sub-micrometer resolution. Commercial laser-scanning microscopes can be upgraded with a SRS module with some important modification. In its simplest form, a SRS microscope can be constructed from a fluorescence laser-scanning microscope by equipping a forward detector and with proper bandpass filters and interfacing the scanning unit of microscope with the detector. Moreover, although standard condensers, which have a NA of ~0.55, suffice to capture a significant portion of the forward- propagating signal, better collection efficiencies are obtained with higher-NA condensers. This is especially important for the SRS techniques, where photothermal and position-dependent interference effects may introduce artifacts in the image (Popov *et al.*, 2012; Chung *et al.*, 2013). Such effects can be mitigated by choosing a high-NA condenser.

Fast image acquisition rates are the prime advantage of SRS imaging over spontaneous Raman microscopy. Using high repetition rate femtosecond pulse trains with average powers in the 10 mW range on the sample produces SRS signals with acceptable SNR in a few microsecond per pixel. For an image with 512 × 512 pixels, this translates in acquisition rates of about a frame per second. Such

imaging speeds are at par with those of linear and multiphoton fluorescence microscopy techniques.

To demonstrate the feasibility of the proposed device, the same sample, used for spectroscopic investigation, is studied. The binary image shown in fig. 4, is single recordings of 512x512 pixels with acquisition time of 16 seconds. The time constant of lock-in amplifier was set to 100μs with a slope of 18dB/oct and 3μV sensitivity. For the process of binarization, an adequate threshold of gray level has been selected with Otsu method (Otsu, 1979).
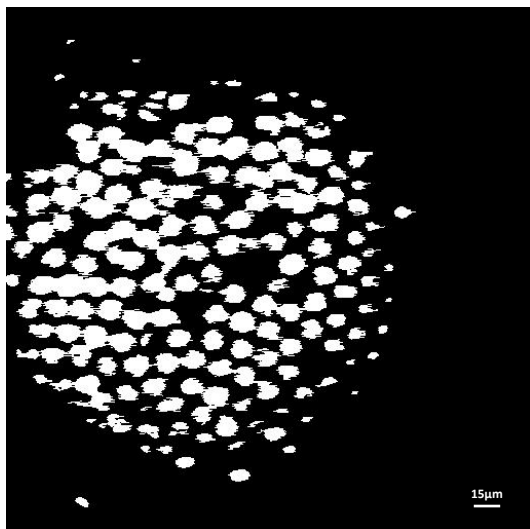
Figure 4: Binary SRS image of 15μm polystyrene beads at 3054cm^{-1} at I$_{pump}$ at 7mW. Scale bar is 15μm.

4 CONCLUSIONS

In this paper, we describe some important connections of SRS with nano- and bio-photonics.

As far as nanophotonics is concerned, experimental investigations of stimulated Raman scattering in nanostructured silicon based materials are compared. Because a theoretical understanding addressing the physical origin of enhanced Raman gain in nanostructured materials remains to be established, in this work we try to give some tiles for the important open question about stimulated Raman scattering at nanoscale. In addition, our results could be an important step towards to silicon based Raman laser.

As far as biophotonics is concerned, femtosecond stimulated Raman spectroscopic and microscopy have been implemented. As a preliminary step for nonlinear microscopy, label free imaging of polystyrene-beads is demonstrated. Next step is to apply this nonlinear optical imaging approach to biological research.

REFERENCES

Cao L., Nabet B., Spanier J. E., 2006, *Enhanced Raman scattering from individual semiconductornanocones and nanowires*, Physical Review Letters, Vol. 96, no. 15, Article ID 157402, pp. 1-4.

Chung C. Y. et al., 2013, *Controlling stimulated coherent spectroscopy and microscopy by a position-dependent phase*, Phys. Rev. A 87(3), 033833.

Ferrara M. A., Donato M. G., Sirleto L., Messina G., Santangelo S., Rendina I., 2008, *Study of Strain and Wetting Phenomena in Porous Silicon by Raman scattering*, Journal of Raman Spectroscopy, Vol. 39, Issue 2, pp. 199-204.

Ferrara M. A., Sirleto L., Nicotra G., Spinella C., Rendina I., 2011, *Enhanced gain coefficient in Raman amplifier based on silicon nanocomposites,* Photonics and Nanostructures – Fundamentals and Applications;pp. 1-7.

Freudiger C. W., et al., 2008, *Label-free biomedical imaging with high sensitivity by stimulated Raman scattering microscopy*, Science 322, 1857–1861.

Fu D., Holtom G., Freudiger C., Zhang X. & Xie X. S., 2013, *Hyperspectral imaging with stimulated Raman scattering by chirped femtosecond lasers*.J. Phys. Chem. B 117, 4634–4640.

Gaponenko S. V., 2002, *Effects of photon density of states on Raman scattering in mesoscopic structures*, Phys.Rev. B, Vol. 65, 140303.

Heritage J. P. and Allara D. L., 1980, *Surface Picosecond Raman Gain Spectra of a Molecular Monolayer,* Chem. Phys. Lett. 74, 507–510.

Kawata S., Inouye Y., Verma P.,2009, *Plasmonics for near-field nanoimaging and superlensing*, Nature Photonics, Vol. 3, no. 7, pp. 388-394.

Levine B. F., Shank C. V., and Heritage J. P., 1979, *Surface Vibrational Spectroscopy Using Stimulated Raman Scattering,* IEEE J. Quantum Electron. QE_15, 1418–1432.

Min W. Freudiger C.W., Lu S., and Xie X. S., 2011, *Coherent Nonlinear Optical Imaging: Beyond*

Fluorescence Microscopy, Annu. Rev. Phys. Chem. 62, pp. 507-530.

Nandakumar P., Kovalev A., and Volkmer A., 2009, *Vibrational Imaging Based on Stimulated Raman Scattering Microscopy*, New J. Phys. 11, 033026–033035.

Nishizawa J., & Suto K., 1980, *Semiconductor Raman Laser*, J. Appl. Phys., Vol. 51,2429-2431.

Otsu N. 1979, *A Threshold Selection Method from Gray-Level Histograms*, IEEE Transactions on Systems, Man, and Cybernetics, Vol. 9, No. 1, pp. 62-66.

Owyoung A., 1978, *Coherent Raman Gain Spectroscopy Using CW Laser Sources*, IEEE J. Quantum Electron.QE_14, 192–203.

Ozeki Y., Dake F., Kajiyama S., Fukui K., & Itoh K., 2009*, Analysis and experimental assessment of the sensitivity of stimulated Raman scattering microscopy,* Opt.Express 17, 3651–3658.

Ploetz E., Laimgruber S., Berner S., Zinth W., & Gilch P., 2007, *Femtosecond stimulated Raman microscopy* .Appl. Phys. B 87,pp.389–393.

Popov K. I. et al., 2012, *Image formation in CARS and SRS: effect of an inhomogeneous nonresonant background medium*, Opt. Lett. 37(4), 473–475.

Refi J. J., 1999, Bell Labs Tech. J., Vol. 4, 246-261.

Rong H. S., Liu A. S., Jones R., Cohen O., Hak D., Nicolaescu R., Fang A., Paniccia M.,2005, Nature, Vol. 433 (7023), 292-294.

Shen Y. R. and Bloembergen N., 1965, *Theory of Stimulated Brillouin and Raman Scattering*, Phys. Rev., Vol. 137, AI787.

Sirleto L., Raghunathan V., Rossi A. and Jalali B., 2004, Electronics Letters 40 (19), 121-122.

Sirleto L., Ferrara M. A., Rendina I., Jalali B., 2006, Applied Physics Letters 88, 211105.

Sirleto L., Ferrara M: A., Rendina I., Basu S. N., Warga J., Li R., Dal Negro L., 2008, *Enhanced stimulated Raman scattering in silicon nanocrystals embedded in silicon-rich nitride/silicon superlattice structures*, Applied Physics Letters, 93, 251104.

Sirleto L., Ferrara M. A., Rendina I., Nicotra G., Spinella C.,2009, *Observation of stimulated Raman scattering in silicon nanocompisties*, Applied Physics Letters, 94, 221106.

Sirleto L, Ferrara M A, Nikitin T, Novikov S, Khriachtchev L., 2012, *Giant Raman gain in silicon nanocrystals*. NATURE COMMUNICATIONS, ISSN: 2041-1723.

Spillane S. M., Kippenberg T. J., Vahala K. J., 2002, Nature, Vol. 415 (6872), 621-623.

Stolen R. H., 2004, *Raman Amplifiers for Telecommunications 1*, (Ed. M. N. Islam) Springer-Verlag, New York, p35.

Wu J., Awnish K. Gupta, Humberto R. Gutierres, Eklund P. C., 2009, Nano Letters, Vol. 9, N. 9, 3252-3257.

Zhang B. P., Shimazaki K., Shiokawa T., Suzuki M., Ishibashi K., Saito R., 2006 Appl. Phys. Lett., Vol. 88 (24),241101-241103.